

Characterization of the Different Stages of Damage Evolution and Crack Growth in Pure Nickel during Ultrasonic Fatigue

Martina Zimmermann^{1,2,a}, Anton Kolyshkin^{3,b}, Christian Stöcker^{4,c} & Hans-Jürgen Christ^{3,d}

¹ Institut für Werkstoffwissenschaft, TU Dresden, Helmholtzstr. 7, 01069 Dresden, Germany

² Fraunhofer-Institut für Werkstoff- und Strahltechnik, Winterbergstr. 28, 01277 Dresden

³ Institut für Werkstofftechnik, Universität Siegen, Paul-Bonatz-Str. 9-11, 57068 Siegen, Germany

⁴ Tital GmbH, Kapellenstrasse 44, 59909 Bestwig, Germany

^a martina.zimmermann@tu-dresden.de, ^b anton.kolyshkin@uni-siegen.de,

^c christian.stoecker@tital.de, ^d hans-juergen.christ@uni-siegen.de

Keywords: very high cycle fatigue (VHCF), crack initiation, crack growth, nonlinear material behavior.

Abstract. In the very high cycle fatigue (VHCF) range fatigue life of non-defect afflicted materials is foremost dominated by crack initiation rather than crack growth. However, this is primarily true for applications where the existence of microcracks/-notches at the surface (e.g. due to manufacturing processes) can be ruled out. In order to assess fatigue life in the VHCF regime with regard to the true nature of early or late failure, the transition line between crack initiation processes, such as transient behavior and microcrack formation, and discontinuous and continuous crack growth have to be characterized as a whole. Using the example of commercially pure nickel Ni 201, fatigue life in the VHCF regime and the various stages of damage evolution up to total failure during ultrasonic fatigue testing are discussed on the basis of two different microstructures, an as-received and a coarse-grained condition. The scatter of fatigue results at stress amplitudes as low as 150 MPa ranges from $\sim 2 \times 10^7$ cycles up to $\sim 2 \times 10^9$ for a run-out sample of the as-received condition. The run-out sample exhibited slipband and microcrack formation at the surface. As a consequence, such microcracks have to be evaluated with regard to their propagation capabilities according to grain orientation and the barrier function of grain boundaries. Moreover, the huge scatter of fatigue results tested at similar stress amplitudes has to be investigated with regard to the stages of crack initiation and crack growth. In order to meet the demand for a distinction between the different stages of damage evolution, ultrasonic fatigue testing is accompanied by the analysis of the feedback signal and its higher harmonics, representing the nonlinear material behavior due to both microstructural changes as well as crack growth effects. The chances and limits of this method for an in-situ characterization of the overall damage process at ultrasonic test frequencies are critically discussed.

Introduction

Although it is of common consensus that fatigue in the VHCF regime is dominated by crack initiation rather than crack growth, even for so-called run-out specimens traces of fatigue damage in the form of microcracks and/or slip band formation can be observed. As a consequence, microcracks have to be evaluated with regard to their propagation capabilities at VHCF relevant load amplitudes in order to be able to define a true fatigue threshold irrespective of the final number of cycles. In the past, crack growth behavior in the VHCF regime was mainly discussed for defect afflicted materials with non-metallic inclusions or pores as crack initiating feature [1-3]. However, early crack growth was discussed lately for quasi defect free materials such as polycrystalline copper or an austenitic-ferritic duplex steel [4,5]. In the case of pure copper, crack propagation requires approximately 100% higher stress/total strain amplitudes than what is needed for the evolution of early fatigue

damage in the form of persistent slip bands and/or microcracks. For the austenitic-ferritic duplex steel, slip band formation in the VHCF regime could be correlated with shear stress maxima deriving from stress concentrations due to elastic anisotropy. The influence of microstructural features in the HCF and VHCF regime was also analyzed for a nickel-base superalloy René 104 [6] and for CMSX-4 [7]. For René 104 a pronounced variation of crack-growth rate of small surface cracks was related to microstructural features of comparable dimensions, where a significant retardation could be observed at $\Sigma 3$ twin boundaries [6]. Crack propagation in CMSX-4 was limited to the $\{111\}$ slip planes with large inclinations to the applied stress axis. Interestingly enough, no significant impact of the microstructural features, such as pores, eutectic pools and carbides typical for this type of single crystal alloy, on crack propagation could be observed [7].

Whenever discussing the effects of microstructural inhomogeneities on the overall fatigue behavior in the VHCF regime and even more so on crack propagation in the stages of early crack growth, deficiencies with respect to 3-dimensional crack growth characterization are mentioned. In-situ observation by means of high brilliance synchrotron radiation is one way to approach this ambitious goal. However, it is a time and manpower consuming technique and only accessible for a limited number of highly experienced researchers. Hence, methodologies which can be directly combined with high frequency fatigue testing under conventional laboratory conditions are of particular interest. One such technique, measurements of the change of second and higher harmonics due to damage accumulation in a fatigued specimen, was applied in combination with an ultrasonic fatigue test system for the first time by A. Kumar et al. for a cast aluminum alloy [8]. Fatigue crack initiation and crack growth was indicated by an increase of a so-called ultrasonic nonlinearity parameter β_{rel} based on the relation between the fundamental and second harmonic displacement signal, which is registered by the displacement transducer of the ultrasonic fatigue system. For the given aluminum cast alloy no fatigue failure was observed for pore sizes of ~ 0.2 mm or below for a stress amplitude of ~ 75 MPa. For samples fatigued up to $1 - 2 \times 10^6$ number of cycles at 100 MPa a change in β_{rel} in the range of 3.5 - 7.5 dB for cracks of a nominal length of 1.7 – 3.23 mm were observed. Regarding the influence of microstructural features, ultrasonic nonlinearity increased more rapidly for specimens with larger secondary dendritic arm spacing.

The correlation between damage accumulation during cyclic deformation and change in ultrasonic nonlinearity was also investigated by A. Kumar et al. for a cast magnesium alloy [9]. This time the authors focused on the characterization of an increase in dislocation density by means of the new in-situ technique. A clear correlation between hardening and softening processes and its corresponding changes in dislocation densities and an increase and decrease of β_{rel} , respectively, could be demonstrated by combined transmission electron microscopy analysis and the registering of the nonlinearity parameter. However, Oruganti et al. discussed in their analysis of the evolution of specific dislocation structures and its effect on the generation of ultrasonic second harmonics (based on ultrasonic attenuation of a failed fatigue sample insonified by means of high power ultrasound piezoelectric transducers acting as input and receiving ends) the influence of homogeneous versus inhomogeneous dislocation arrangements and the material basic microstructure [10]. According to their assumptions β_{rel} can both increase or decrease with increasing dislocation density depending on the interaction of dislocations with microstructural features such as pile-ups of dislocations at precipitates.

Material and Experimental Setup

Fatigue testing was carried out on commercially pure Nickel Ni 201 by means of an ultrasonic fatigue testing system (details see [12]). Undesirable heating of the specimens due to the high test

frequencies was avoided by actively cooling the samples and pulse/pause test sequences. Fatigue crack growth was registered in-situ, using an optical microscope and a CCD-camera system, allowing triggered photographic images of the crack front at the surface for specially designed fatigue crack growth specimens with two different geometries, a bulk sample (Fig. 1a) and microfoils in combination with a carrier sample (Fig. 1b) during fatigue testing. In addition, fatigue crack growth was monitored on cylindrical hourglass-shaped samples with a critical cross section diameter of 3 mm (Fig. 1c), which were also successfully used for overall ultrasonic fatigue testing. In this case, crack growth was quantified by interrupted testing combined with optical inspections using confocal laser microscopy.

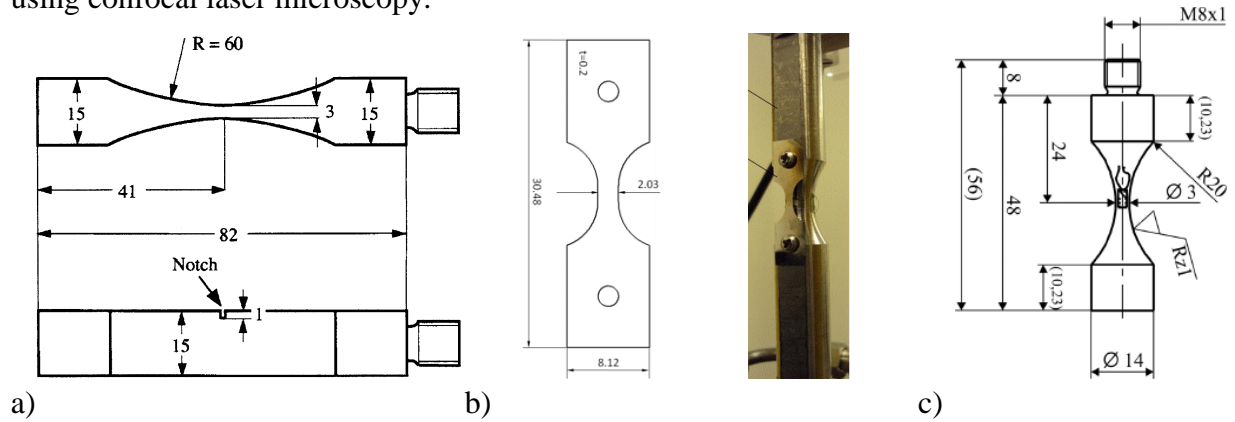


Fig. 1: Geometries for fatigue crack growth testing using an ultrasonic fatigue test system: a) bulk crack growth sample, b) microfoil and carrier specimen and c) conventional ultrasonic fatigue test specimen (geometries are not drawn to consistent scale).

With the microfoils thickness being of the order of $\sim 200 \mu\text{m}$, coarse-grain annealing of the as-received condition of Ni 201 resulting in an average grain size of $\sim 410 \mu\text{m}$ (Fig. 2a) allowed crack growth monitoring in quasi single-crystal structures over the sample thickness in a polycrystalline material. Due to the annealing process the original status of dislocation density and arrangement of the original wrought material was altered, which is reflected in the different cyclic deformation curves for each condition as is depicted in Fig. 2b. A conventional servo-hydraulic test system was used in order to generate the cyclic deformation curves, as the ultrasonic test system does not allow continuous strain measurements by means of strain gauges due to its test frequencies around 20 kHz. The use of the conventional test system limited the registration of the cyclic deformation curve to a number of cycles $N \leq 2 \times 10^6$.

In order to characterize the cyclic deformation behavior and damage accumulation for amplitudes and number of cycles in the VHCF regime, the earlier described technique of nonlinear ultrasonics was applied. The system setup, consisting of the ultrasonic fatigue test system together with a digital oscilloscope and a data acquisition software, allows to analyze and document the feedback signal in form of sinusoidal mechanical waves with defined amplitudes, originally initiated by the ultrasonic transducer and measured through the vibration gauge during fatigue testing. As described earlier on, fatigue damage and crack growth behavior can be described by the ultrasonic nonlinearity parameter β_{rel} , based on the amplitudes of the first and second harmonics (a_1 and a_2), which are transformed into an amplitude spectra by means of fast fourier transformation (Fig. 3). The parameter β_{rel} is defined by the equations given in Fig. 3 and is based on the amplitudes of the first and second harmonics a_1 and a_2 , the fundamental frequency ω_0 , the ultrasonic wave velocity c and the propagation distance x .

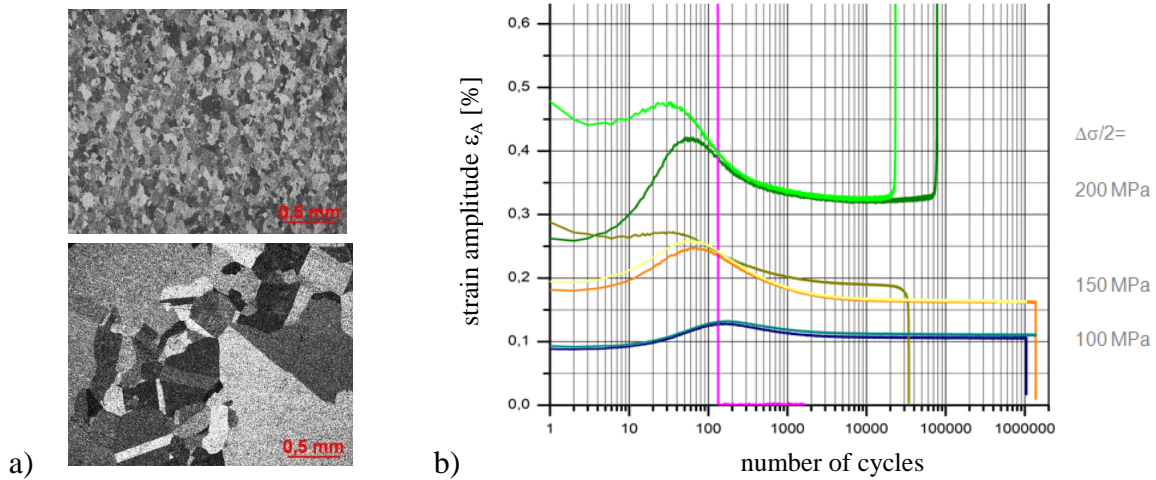


Fig. 2: Micrographs of Ni 201 in the as-received and coarse-grained condition (a) and corresponding cyclic deformation curves (b).

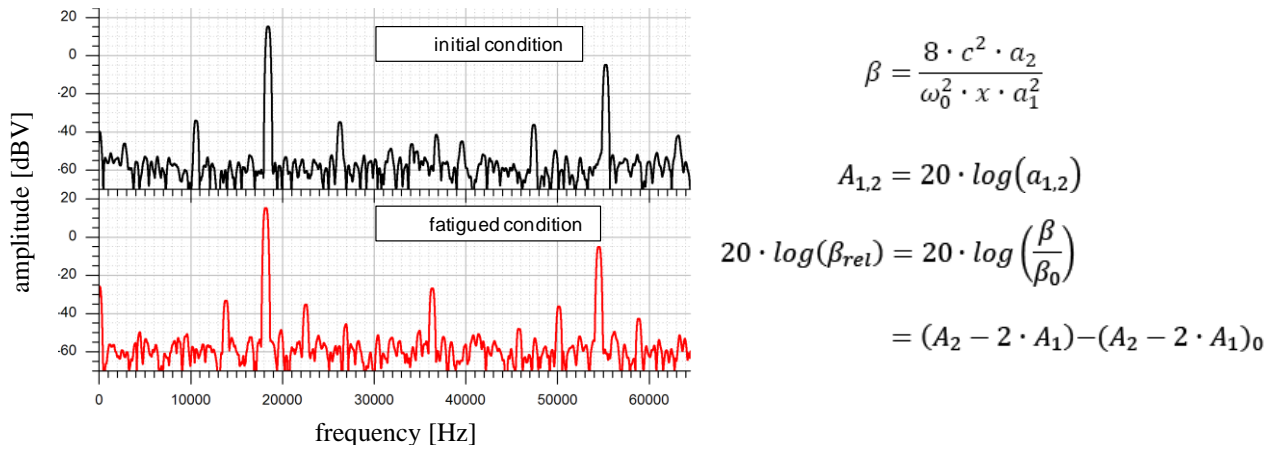


Fig. 3: Amplitude spectrum registered during ultrasonic fatigue testing with a significant change of the second harmonic.

Results and Discussion

The results of fatigue tests performed on Ni 201 are depicted in Fig. 4. Even at an amplitude of $\sigma_A = 150$ MPa failure was observed at a number of cycles as high as $N_f = 8.9 \times 10^8$ cycles. Moreover, slip band formation occurred in isolated grains at the surface of run-out specimens, but did not exceed grain boundaries with increasing number of cycles. The results of an electron backscattered diffraction (EBSD) analysis identified those grains with slip bands as grains with a high Schmid factor and surface roughening started preferably at grain boundary triple junctions. In addition to the surface roughening, the evolution of intergranular as well as transgranular microcracks could be observed in run-out specimens, as is depicted in Fig. 4. Comparing fatigue results derived by means of high frequency testing with additional tests at frequencies of $f = 135$ Hz and 75 Hz confirmed that the overall fatigue behavior of Ni 201 does not show any strain rate sensitivity under the given testing conditions.

Fatigue crack growth tests revealed crack growth as early as at a stress intensity factor of $\Delta K = 3.54$ MPa $\sqrt{\text{m}}$ at minimum growth rates of 10^{-12} m/cycles. A slight tendency towards a higher threshold value for the coarse-grained condition could be observed. As the starter notch is relatively obtuse with regard to the length of the initial crack length (notch radius ~ 30 μm and resolution for crack growth $\sim 2\text{-}5$ μm), even lower threshold values are assumed for a sharper starter notch.

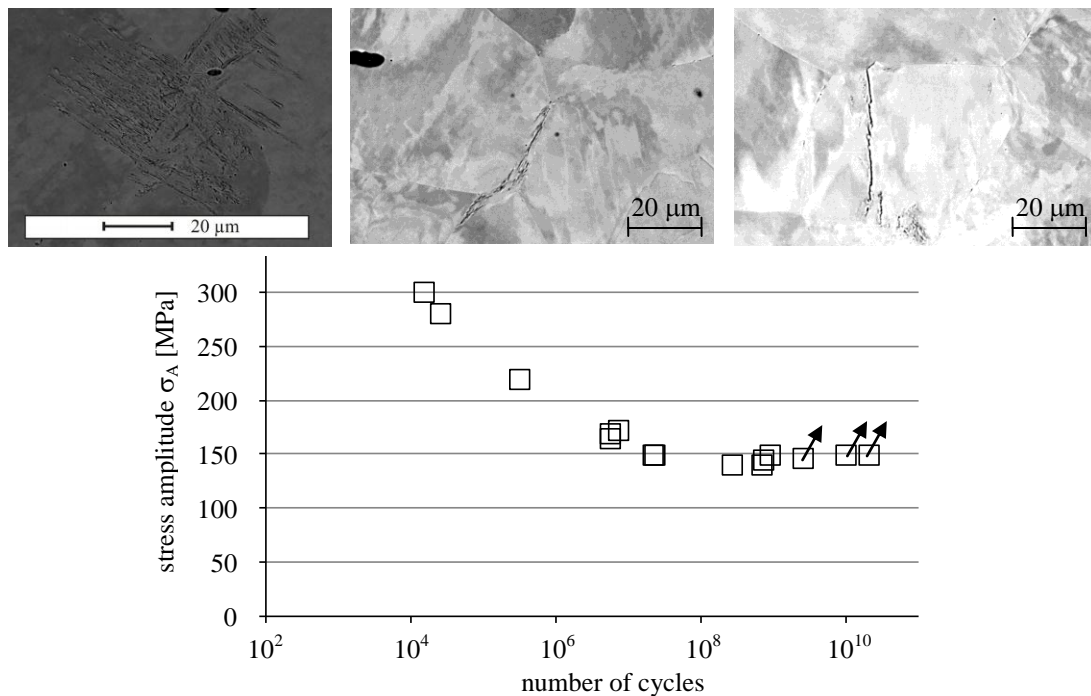


Fig. 4: Fatigue results in the HCF and VHCF regime for Ni 201, surface roughening and microcrack formation in run-out specimens.

A comparison of the crack paths for the as-received and the coarse-grained condition reveals a much more pronounced bifurcation level of the coarse-grained microstructure in contrast to the almost straight and perpendicular path of the as-received condition. However, both conditions are not limited to stadium II crack growth behavior but reveal an influence of the microstructure for the tested very low crack growth rates at very low amplitudes. Hence, it is astonishing that even in the coarse-grained condition stadium I crack growth is not solely restricted to single slip mode.

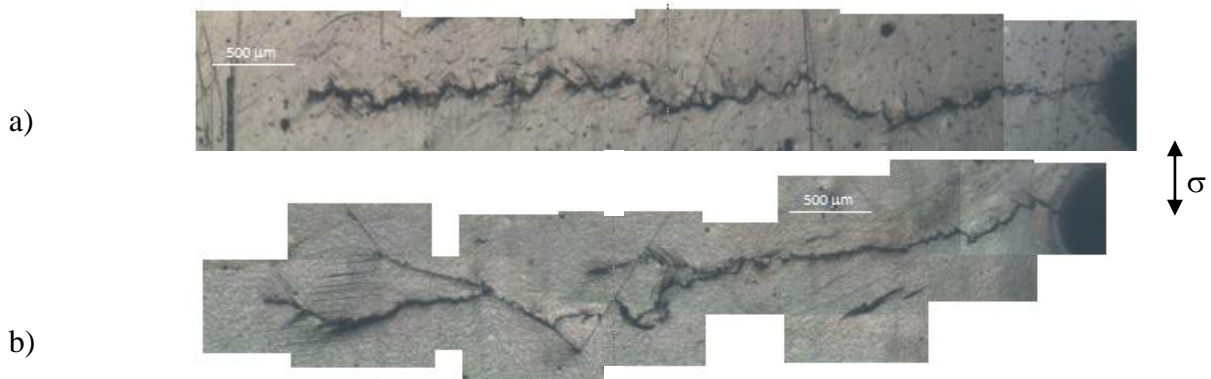


Fig. 5: Crack path in bulk samples Ni 201 for fatigue crack growth tests in the VHCF regime in a) the as-received and b) the coarse-grained condition.

Provided that for the given crack growth samples and the experimental setting linear elastic fatigue crack growth in mode I can be assumed, a threshold of $\Delta K \approx 3.54 \text{ MPa}\sqrt{\text{m}}$ and an overall fatigue limit of 145 MPa for $N = 10^9$ allows a critical crack length of a $\approx 0.171 \text{ mm}$ according to the Kitagawa-Takahashi diagram. Hence, the microcracks depicted in Fig. 4c + d can be classified as uncritical, non-propagating cracks. But with threshold values and growth rates varying significantly for the overall number of specimens tested, a closer investigation of the influence factors, and here in particular the grain size and morphology had to be followed up.

For the coarse-grained condition a change in crack path was often preceded by a halt of the crack growth and afresh crack propagation could only be reactivated by increasing the stress amplitude. A direct correlation between discontinuous crack propagation and grain morphology was observed in the microfoil fatigue crack growth samples, showing that a cluster of smaller grains with different crystallographic orientation lead to a pronounced crack growth retardation while in favourably oriented, large grains an increase of crack growth rate could be observed, see a comparison of crack growth rate, crack path and a superimposed EBSD analysis depicted in Fig. 6. However, a direct correlation of the crack growth behavior and the grain morphology was only feasible because of the microfoils thickness of $\sim 200 \mu\text{m}$. In order to further study the transition stage between crack initiation and crack growth behavior under VHCF testing conditions in bulk samples, the nonlinear ultrasonics technique was chosen as indirect characterization method. The question at hand is, whether this method allows a characterization of the damage evolution during VHCF loading sensitive enough to gain further insights into the influence of microstructure on interior crack propagation.

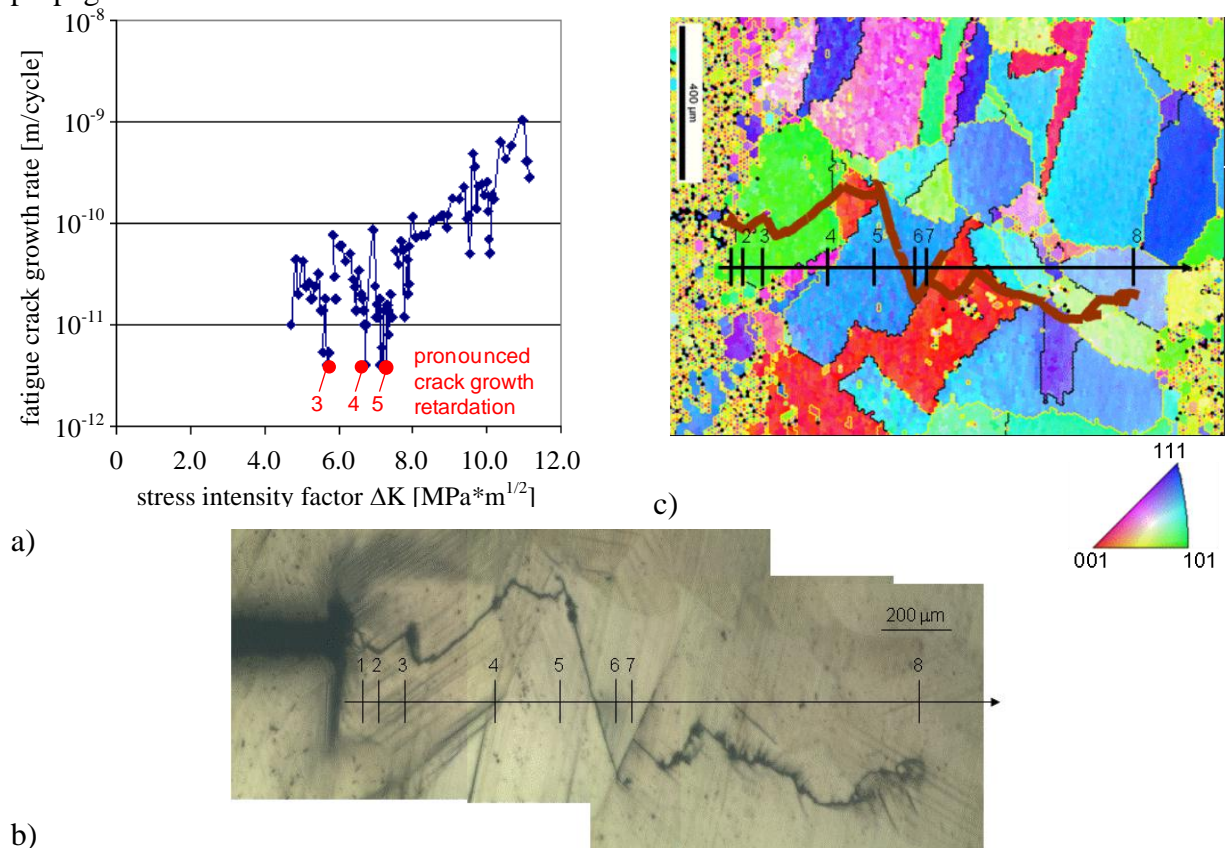


Fig. 6: Fatigue crack growth rate for a coarse-grained microfoil Ni 201 (a), its corresponding crack path (b) and the underlying grain morphology (c).

Fig. 7a depicts examples for the course of the relative nonlinearity parameter β_{rel} during fatigue testing of cylindrical fatigue samples. No starter notches were introduced in those samples, hence crack initiation occurred naturally during cyclic loading. A sample in the as-received condition was tested at a stress amplitude of 200 MPa, which according to the S-N-curve given in Fig. 4a can clearly be attributed to the transition range between HCF and VHCF. A surface crack of a $\approx 0.25 \text{ mm}$ became visible after $N = 10^6$ numbers of cycles and was signalled even earlier by an increase of β_{rel} . Subsequently, crack growth was accompanied by a continuous increase of β_{rel} from around 3 dB up to approximately 7 dB resulting in a final crack length of a $\approx 1.2 \text{ mm}$. An EBSD

analysis of the grain morphology around the crack path (Fig. 7b) reveals similar crack growth behavior as described before for the as-received condition, showing both transgranular as well as intergranular cracking and only minor crack path branching.

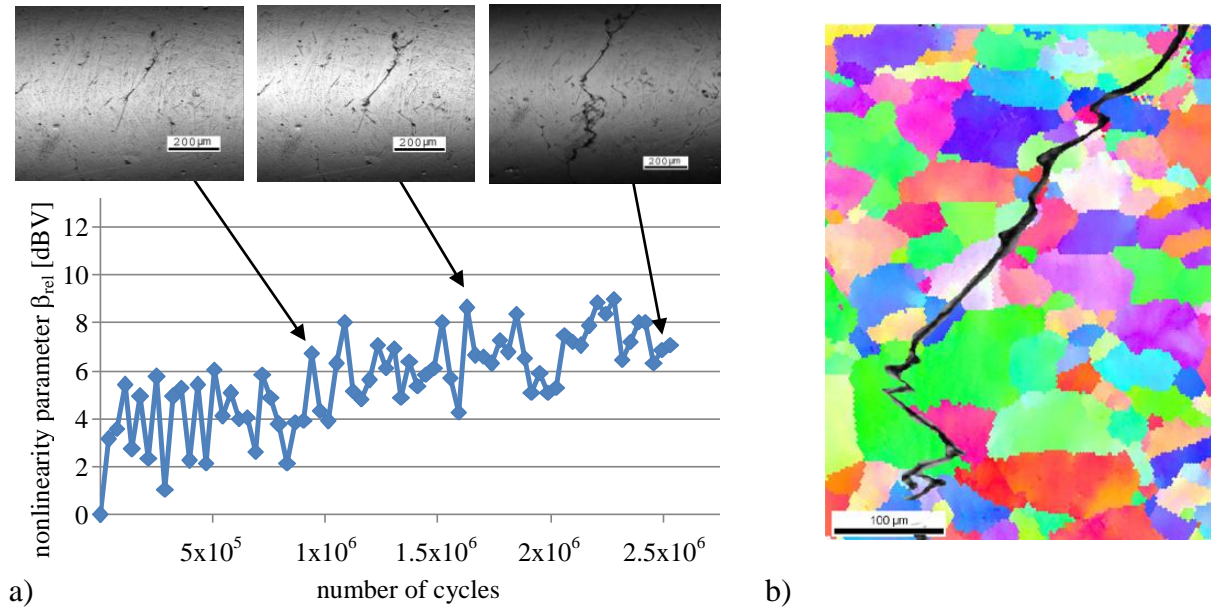


Fig. 7: The relative nonlinearity parameter β_{rel} and the evolution and growth of a fatigue microcrack in an as-received sample during cycling at 200 MPa (a) and EBSD-scan around the crack path (b).

In contrast to the results presented for the as-received condition, the correlation between the course of β_{rel} and crack initiation and early crack growth for the coarse-grained condition is rather ambiguous. A sample was fatigued at 120 MPa, a stress amplitude well below the fatigue limit of 145 MPa for $N = 10^9$, and microcrack formation was detected at $N = 2.9 \times 10^7$ numbers of cycles with a crack length of a ≈ 0.15 mm, propagating to a ≈ 0.6 mm for the overall number of cycles $N = 5.1 \times 10^7$. The test was cancelled at that point, while no change in resonance frequency (the classical failure criterion for ultrasonic fatigue testing) was detectable. The course of β_{rel} for the sample does neither change significantly during the crack initiation phase nor during crack growth (Fig. 8a). Moreover, hardening and softening, as would have been expected for the coarse-grained condition and the given stress amplitude based on the cyclic deformation curve given in Fig. 2b, for a number of cycles up to $N \approx 10^4$ is also not reflected in a change of β_{rel} . However, a minor decrease of β_{rel} can be perceived between $N \approx 1 \times 10^7$ and 3.5×10^7 .

According to an EBSD analysis of the microstructure around the microcrack (Fig. 8b), crack initiation started at a grain boundary triple junction and the crack propagated intergranularly with two competing crack paths. Hence, the slight change of β_{rel} might be related to the activation of the second crack path. However, this assumption does not match the insensitivity of β_{rel} regarding a change in dislocation density as can be assumed by the cyclic hardening and softening observed for the applied stress amplitudes. A preliminary evaluation of the nonlinearity parameter as indirect methodology to characterize the different stages of damage evolution as was proclaimed by various authors cannot yet be confirmed for the quasi defect free material analyzed in the given study. Tests with a sample being endowed with a starter notch that has similar dimensions as a microcrack introduced by means of focused ion beam technology are planned in order to further elucidate the effect of crack path and grain morphology on the course of β_{rel} as assumed for the coarse-grained sample.

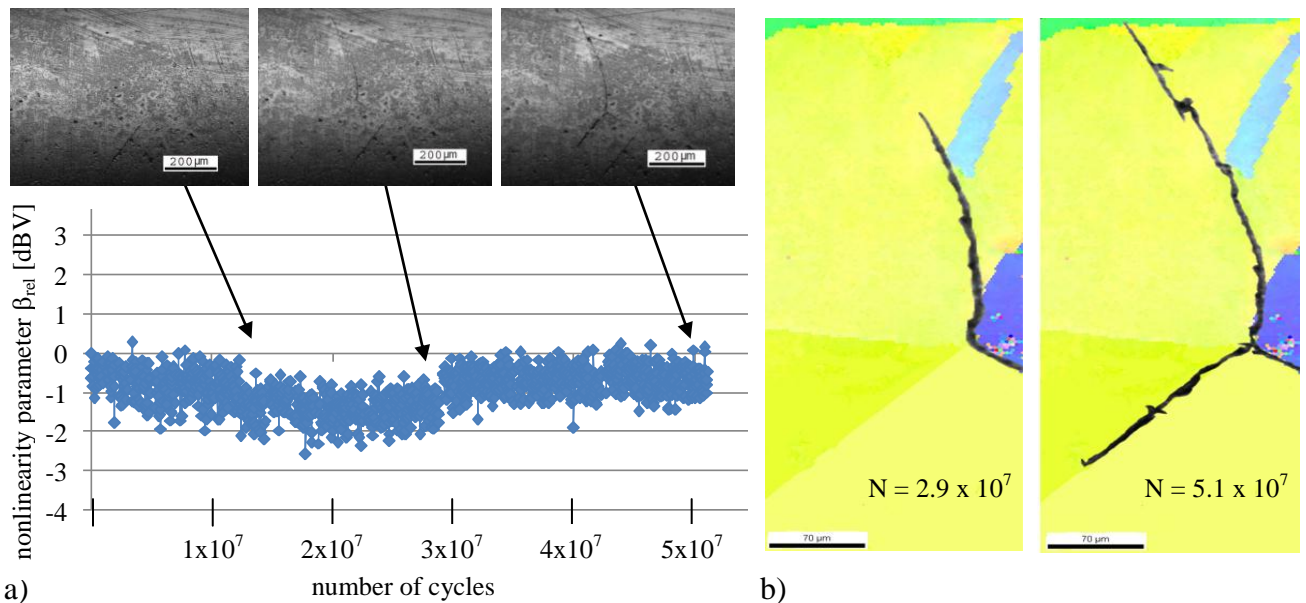


Fig. 8: The relative nonlinearity parameter β_{rel} and the evolution and growth of a fatigue microcrack in a coarse-grained sample during cycling at 120 MPa (a) and EBSD-scan around the crack path (b).

Conclusions

Overall fatigue behavior and fatigue crack growth in the VHCF regime was analysed for commercially pure Nickel Ni 201 in an as-received and coarse-grained condition. Slip band and microcrack formation was observed even in run-out specimens favorably initiating at grain boundary triple junctions. Crack growth occurred at a stress intensity factor as low as $\Delta K \approx 3.54$ at minimum growth rates of 10^{-12} m/cycles. Crack growth retardation and bifurcation was more pronounced in the coarse-grained microstructure and could be correlated with grain morphology. Comparing the course of the nonlinearity parameter β_{rel} for the two microstructures during fatigue crack growth testing did not yet lead to unambiguous results. For the as-received condition the evolution and early crack growth stood in good correlation with the continuous increase of β_{rel} . However, for the coarse-grained condition, a significant change in β_{rel} was neither observed in connection with crack growth nor with inelastic material behavior as a result of cyclic hardening and softening. Hence, monitoring the nonlinearity parameter β_{rel} as indirect methodology to characterize the different stages of damage evolution cannot yet be ultimately confirmed as suitable technique.

References

- [1] S. Stanzl-Tschegg, B. Schönbauer: Proc. Eng. Vol. 2 (2010), p. 1547.
- [2] C. Bathias: Gigacycle Fatigue Properties of Bearing Steels in: ASTM STP 1524 (Ed.: J. M. Beswick), ASTM International, West Conshohocken (2010) p. 160.
- [3] Y. Murakami: Metal Fatigue: Effects of Small Defects & Nonmetallic Inclusions, Elsevier, New York (2002).
- [4] S. Stanzl-Tschegg, B. Schönbauer: Int. J. Fatigue Vol. 32 (2010), p. 886.
- [5] U. Krupp, A. Giertler, M. C. Marinelli, H. Knobbe, H.-J. Christ, P. Köster, C.-P. Fritzen, S. Herenu, I. Alvarez-Armas in: Proc. of the 5th Int. Conf. on VHCF, edited by C. Berger, H.-J. Christ, DVM, Berlin (2011), p. 127.
- [6] Y. Gao, J.S. Stölken, M. Kumar, R.O. Ritchie: Acta Mater. Vol. 55 (2007), p. 3155.
- [7] L. Liu, N.S. Husseini, C.J. Torbet, D.P. Kumah, R. Clarke, T.M. Pollock, J.W. Jones: J. Eng. Mater. Technol. Vol. 130 (2008), p. 021008-1-6.
- [8] A. Kumar, C.J. torbet, T.M. Pollock, J.W. Jones: Acta Mater. Vol. 58 (2010) p. 2143.
- [9] A. Kumar, R.R. Adharapurapu, J.W. Jones, T.M. Polock: Scripta Mater. Vol. 63 (2011) p. 65.
- [10] R.K. Oruganti, R. Sivaramanivas, T.N. Karthik, V. Kommareddy, B. Ramadurai, B. Ganesan, E.J. Nieters, M.F. Gigliotti, M.E. Keller, M.T. Shyamsunder: Int. J. Fatigue Vol. 29 (2007) p. 2032.